Ecological Indicators 130 (2021) 108111

Contents lists available at ScienceDirect

Ecological Indicators

journal homepage: www.elsevier.com/locate/ecolind

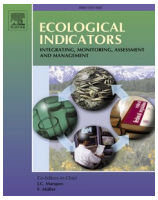

Evaluating different methods for retrieving intraspecific leaf trait variation from hyperspectral leaf reflectance

Kenny Helsen [a,b,1,*], Leonardo Bassi [c,1], Hannes Feilhauer [d,e], Teja Kattenborn [d], Hajime Matsushima [f], Elisa Van Cleemput [g], Ben Somers [h], Olivier Honnay [a]

[a] Plant Conservation and Population Biology, Biology Department, KU Leuven, Kasteelpark Arenberg 31, 3001 Leuven, Belgium
[b] Institute of Ecology and Evolutionary Biology, National Taiwan University, No. 237, Zhoushan Road, Da'an District, Taipei 106, Taiwan
[c] Systematic Botany and Functional Biodiversity, Institute of Biology, Leipzig University, Johannisallee 21-23, 04103 Leipzig, Germany
[d] Remote Sensing Centre for Earth System Research, Leipzig University, Talstr. 35, 04103 Leipzig, Germany
[e] Department of Remote Sensing, Helmholtz-Centre for Environmental Research - UFZ, Permoserstr. 15, 04318 Leipzig, Germany
[f] Research Faculty of Agriculture, Hokkaido University, Kita 9 Nishi 9, Kita-ku, Sapporo 060-8589, Japan
[g] Institute of Arctic and Alpine Research, University of Colorado, 4001 Discovery Drive, Boulder, CO 80303, USA
[h] Division of Forest, Nature and Landscape, KU Leuven, Celestijnenlaan 200E, 3001 Leuven, Belgium

ARTICLE INFO

Keywords:
Intraspecific trait variation
Leaf dry matter content
Leaf mass per area
Leaf water content
Equivalent water thickness
Partial least squares regression (PLSR)
PROSPECT

ABSTRACT

Leaf mass per area (LMA), leaf dry matter content (LDMC) and leaf water content/ equivalent water thickness (EWT) are commonly used functional plant traits in ecology. Whereas spectroscopy has recently proven to be a powerful tool to collect such functional trait information across large scales, it remains unclear whether these reflectance-based trait predictions are accurate enough to reliably model trait variation at the intraspecific level (i.e. across individuals of one species). We explored the potential of hyperspectral leaf reflectance-based methods to predict LMA, LDMC and EWT at the intraspecific level for two herbs (*Hieracium umbellatum* and *Jacobaea vulgaris*) and two shrubs (*Rosa rugosa* and *Rubus caesius*), based on 2400 leaf samples. More specifically we tested i) inversion of the PROSPECT-D radiative transfer model, ii) a generic PLSR approach using the multibiome LMA PLSR model and iii) a data-specific PLSR approach at the species level. For the latter approach we furthermore assessed both model transferability across species and the trade-off between sample size and model accuracy. Although the PROSPECT-D model inversion and the multibiome LMA PLSR model were relatively accurate for intraspecific LMA predictions of shrubs ($R^2 > 71$ and 76%, respectively, however NRMSE = 33–47%), their performance was lower for herbs ($R^2 < 61\%$, NRMSE = 28–50%). PROSPECT-D was furthermore slightly less successful in retrieving EWT at the intraspecific level ($R^2 < 70\%$, NRMSE = 16–43%), and unsuccessful in retrieving LDMC through combining LMA and EWT inversion results ($R^2 < 10\%$, NRMSE = 9–192%). The highest correlation accuracy was obtained for all three traits with the species-specific PLSR models ($R^2 > 70\%$, NRMSE < 10%). If high predictive accuracy is needed, we thus suggest the use of species-specific PLSR models. The training of species-specific PLSR models comes at the cost of a needed sample size of 100–160 leaves however, depending on the trait. Although transferability of species-specific PLSR models seems limited overall, our results suggest potentially high transferability across herbaceous species.

1. Introduction

Leaf (dry) mass per (fresh) area (LMA) and leaf dry matter content (LDMC), the oven-dry mass of a leaf divided by its water-saturated fresh mass, are among the most commonly used functional leaf traits in ecological research (Garnier et al., 2004; Poorter et al., 2009; Pérez-Harguindeguy et al., 2013). Their frequent use can be attributed to their impact on and response to a wide range of ecological processes (Westoby, 1998; Wilson et al., 1999; Poorter et al., 2009). For example, both traits are considered to be part of the global leaf economics spectrum (Wilson et al., 1999; Wright et al., 2004; Pierce et al., 2017) and consequently link up with plant-level responses to both abiotic drivers

* Corresponding author at: Plant Conservation and Population Biology, Biology Department, KU Leuven, Kasteelpark Arenberg 31, 3001 Leuven, Belgium.
E-mail address: kenny.helsen@kuleuven.be (K. Helsen).
[1] shared first author

https://doi.org/10.1016/j.ecolind.2021.108111
Received 15 January 2021; Received in revised form 2 August 2021; Accepted 13 August 2021
Available online 27 August 2021

such as drought (Hodgson et al., 2011; Wellstein et al., 2017) and biotic drivers such as competition (Kunstler et al., 2016). A plethora of ecosystem functions have also been linked to LMA and LDMC, including primary production (Garnier et al., 2004; Smart et al., 2017) and litter decomposition (Garnier et al., 2004; Tao et al., 2019). Alternatively to LDMC, leaf water content is sometimes measured as an expression of moisture content. When leaf water content is expressed per leaf area (mg cm^{-2}), it is often referred to as equivalent water thickness (EWT), and can be transformed to LDMC through LMA (EWT = (LMA × $LDMC^{-1}$) - LMA). As a functional trait, EWT has been shown to relate to a plant's thermal regulation, drought resistance and flammability (Zeiger, 1983; Lawlor and Cornic, 2002). Accurate assessments of both LMA and EWT are moreover important to monitor 'fuel moisture content' (=EWT LMA^{-1}, mg mg^{-1}), an important ecosystem proxy related to fire risk assessment (Yebra et al., 2013).

Assessing functional trait patterns across large spatial and temporal scales is logistically challenging. To alleviate these constrains, spectroscopy has proven to provide a powerful tool to collect large-scale functional trait information (Gamon et al., 2019). This involves recording specific light absorption and scattering features of plants across a number of spectral bands that can be linked to traits such as LMA, LDMC and EWT. Semimechanistic approaches, such as radiative transfer models, have proven successful at extracting functional trait information from leaf and canopy reflectance. These models are termed 'semimechanistic' because they combine physically existing links between certain traits and spectral properties with empirically derived specific absorption coefficients for these physical links (Jacquemoud and Baret, 1990; Jacquemoud et al., 2009; Kattenborn and Schmidtlein, 2019). While these models take advantage of the straightforward and causal correlation between certain traits (e.g. EWT) and their spectral absorption features, for other traits (e.g. LMA) these links are more complex, because multiple structural components underlie their spectral retrievability (Cheng et al., 2014). While radiative transfer models such as PROSPECT do not allow direct quantification of LDMC, theoretically this trait could be indirectly estimated from EWT and LMA, both of which are included in the PROSPECT model (LDMC = LMA/(LMA + EWT)) (Féret et al., 2019).

Next to semimechanistic, also purely empirical statistical approaches have been adopted to quantify traits. The mathematically most straightforward statistical methods are known as 'vegetation indices' (VIs), which consist of simple univariate regression methods that combine a small number of spectral bands (Homolová et al., 2013; Verrelst et al., 2015). Advances in more complex multivariate statistical modelling techniques, such as partial least squares regression (PLSR) (Wold et al., 1983) have, however, also resulted in accurate extraction of functional trait proxies from hyperspectral data (Verrelst et al., 2015; Verrelst et al., 2019). The recently developed multibiome PLSR leaf-reflectance based prediction model for LMA nicely illustrates the potential of these statistical modelling techniques (Serbin et al., 2019). This model was trained on 2478 leaf samples from > 176 species and showed high model accuracy across biomes in the Americas ($R^2 = 0.89$) (Serbin et al., 2019).

In most studies exploring the accuracy of spectrally-derived leaf-level LMA, LDMC and EWT predictions, validation is usually performed across species or vegetation types and thus across relatively large trait ranges (e.g. Wang et al., 2011; Asner et al., 2011; Asner et al., 2015; Singh et al., 2015; Ali et al., 2017; Serbin et al., 2019). Whether such trait models are accurate enough to reliably reflect more subtle trait differences at the intraspecific level (intraspecific trait variation, ITV, i.e. across individuals of one species) remains unclear (Girard et al., 2020; however see Colombo et al., 2008; Feilhauer et al., 2018). There is nonetheless a need for methods allowing fast and correct assessment of trait values at the intraspecific level, since ecological research is increasingly demonstrating the extent (Messier et al., 2010; Siefert et al., 2015) and importance of ITV in explaining both community ecological processes (e.g. Jung et al., 2014; Bennett et al., 2016) and ecosystem functioning (e.g. Breza et al., 2012; Helsen et al., 2018).

Whether a semimechanistic or a statistical modelling approach is most promising to accurately retrieve trait values at the intraspecific level remains unclear, due to the trade-offs presented by their respective advantages and disadvantages. Semimechanistic models have the advantage that they are mainly based on relatively well-understood mechanistic relationships between the retrieved traits and spectral reflectance (Jacquemoud et al., 2009; Féret et al., 2019). Their retrieval accuracy, however, depends on the physical realism of the model and can often be improved through prior information on the expected trait variation range (Verrelst et al., 2015). Specifically in the context of species-specific models (assessing ITV), this could result in reduced sensitivity to subtle variation, potentially impacting their predictive accuracy. Statistical models, on the other hand, are not guaranteed to present solutions linked to the true physical relationship between traits and leaf optical properties and usually lack a physical basis to interpret the model's parameters. This increases the chance of species-specific models that lack transferability (Verrelst et al., 2015; Féret et al., 2019). In addition, unlike semimechanistic models, statistical models require some actual trait measurements for calibration. However, statistical models do allow trait quantification of a larger suite of functional traits and effectuate this through complex and indirect relationships. This enables these methods to take advantage of co-variation between different functional traits within a certain dataset, potentially increasing model sensitivity and retrieval accuracy at the intraspecific level (Atzberger et al., 2015; Verrelst et al., 2019).

In this study we explore the potential of hyperspectral leaf reflectance data to reliably predict LMA, LDMC and EWT at the intraspecific level for two herbs and two shrubs. The number of studies exploring the accuracy of spectrally-derived LMA, LDMC and EWT predictions is less extensive for (herbaceous) grass- and shrubland species, since most work has focused on forests (Homolová et al., 2013; Van Cleemput et al., 2018; however see Roelofsen et al., 2014; Serbin et al., 2019; Girard et al., 2020). In total, we measured these traits for 2399 leaves across the four species and additionally obtained the hyperspectral reflectance of each of these leaves. For three of these species; *Hieracium umbellatum*, *Jacobaea vulgaris* and *Rubus caesius*, all samples were collected along the Belgian North Sea coast. For the fourth study species, *Rosa rugosa*, half of the samples were collected along the Belgian North Sea coast in its invaded range, and the other half along the sea of Japan coast in Northern Japan, in the species' native range. Since many invasive species exhibit different traits between their native and invaded ranges (e.g. Zou et al., 2007; Chun et al., 2009), this offered the opportunity to evaluate model transferability within a species. We addressed the following research questions:

- Is the inversion of the PROSPECT semimechanistic radiative transfer model accurate enough to reliably quantify LMA, EWT and (indirectly) LDMC at the intraspecific level from hyperspectral leaf reflectance?
- Can PLSR models trained across a large range of species (cf. the Serbin et al. (2019) LMA model) reliably predict traits at the intraspecific level?
- Does species-specific statistical PLSR modelling enable an accurate quantification of LMA, LMDC and EWT at the intraspecific level?
- Specifically for *R. rugosa*, can the PLSR model trained for the invasive range provide correct trait predictions for the native range? And more generally, are the species-specific PLSR models generalizable across the other study species?
- How strong is the trade-off between training dataset size and model accuracy, in other words what is the minimum sample size needed for an adequate predictive PLSR model?

2. Materials and methods

2.1. Trait and reflectance data acquisition

Sampling was performed during June 2018 in the coastal sand dunes along the 60 km long Belgian North Sea coast (51.23°N, 2.90°E). In total we established fifty 3 m × 3 m vegetation plots containing a representative selection of the abiotic and biotic variation of coastal dune grasslands in Belgium. In each of these plots we focused on four plant species typical of coastal sand dune grasslands, two dominant clonal woody species; *Rosa rugosa* Thunb. and *Rubus caesius* L., and two subordinate herbs; *Jacobea vulgaris* Gaertn. and *Hieracium umbellatum* L. Since *R. rugosa* is an invasive species in Belgium (Bruun, 2005), we performed an additional sampling for *R. rugosa* during June 2019 along the 30 km long Ishikari sand dunes along the sea of Japan near the city of Sapporo on the northern Japanese island of Hokkaido (43.25°N, 141.35°E). This area is part of the species' native range and the most likely original source of introduction of the Belgian *R. rugosa* populations (Kelager et al., 2013). During this sampling campaign, another twenty-five 3 m × 3 m vegetation plots were established, all containing *R. rugosa* populations. Note that *R. rugosa* was in the same phenological stage in both ranges during sampling (early flowering onset).

Leaf mass per area (LMA, mg cm^{-2}, the inverse of specific leaf area) and leaf dry matter content (LDMC, mg mg^{-1}) were measured for each study species using the protocol of Pérez-Harguindeguy et al. (2013). For each plot × species combination we measured both traits for 15 individuals. Leaf area and fresh weight were measured within 48 h of collection on leaves rehydrated in wet Ziploc bags and stored at 5 °C, using a Canoscan LiDe 120 flatbed scanner (Canon, Japan) and a precision balance (0.1 mg accuracy), respectively. Leaf dry weight was measured after minimum 48 h oven-drying at 70 °C. Equivalent water thickness (EWT, mg cm^{-2}) was subsequently calculated for each leaf sample as (fresh weight – dry weight)/area. The extent of ITV was quantified for each species and trait as the coefficient of variance, i.e. the standard deviation divided by the trait mean.

Before trait processing, we measured the directional hyperspectral reflectance within 48 h of collection of the adaxial surface of each field collected, Ziploc-bag stored (i.e. rehydrated) leaf. Reflectance was measured using a SVC HR-1024i^{TM} spectroradiometer equipped with a plant probe (leaf clip assembly), covering the 350–2500 nm spectral range and a resampled spectral resolution of 1 nm (Spectra Vista Corporation, NY, USA). We used the Spectralon and dark background provided with the spectroradiometer for measurements. Prior to data analysis we removed the 350–400 nm and 2450–2500 nm noise windows and applied a Savitzky-Golay filter with a moving window of 45 nm using the 'hsdar' R package version 0.7.2. (Savitzky and Golay, 1964; Lehnert et al., 2018).

Note that not all study species occurred in each plot, and that due to insufficient quality, 138 (5.4%) leaves and leaf spectra were removed from the final dataset, resulting in a total dataset of trait and spectral leaf data for 669 plants for *R. caesius*, 657 plants for *J. vulgaris* and 344 plants for *H. umbellatum*, all from Belgium. For *R. rugosa* the final dataset contained 371 plants from Belgium (the invaded range) and 358 plants from Japan (the native range).

2.2. Semimechanistic model-based trait estimation

We inverted the PROSPECT-D radiative transfer model to quantify LMA and EWT for all leaf level spectra (Féret et al., 2017; Féret et al., 2019). PROSPECT-D was chosen over previous PROSPECT versions because it has improved trait parametrization based on a larger database, and on the inclusion of anthocyanins (Féret et al., 2017). We tested five approaches for the PROSPECT-D inversion. First, we used the 'direct inversion method' (iterative optimization) with the 'optim' function, based on the Matlab-code of Féret et al. (2008), implemented in the 'hsdar' R package. Second, we used a 'modified direct inversion method' which first estimates the leaf structure parameter Ns directly from the reflectance spectra using equation 4 of Spafford et al. (2021), followed by PROSPECT-D inversion using only the 1700 to 2400 nm spectral domain for LMA and EWT estimation. These modifications have recently shown to improve LMA and EWT retrieval at the interspecific level across a large combined spectral dataset, and are implemented in the 'Invert_PROSPECT_OPT' function of the 'prospect' R package (Féret et al., 2019; Spafford et al., 2021). Third, we used the 'wavelet inversion method' of Kattenborn et al. (2019), which combines wavelet analysis with a look-up-table (LUT) creation. Absorption processes in leaves act in overlapping wavelength regions, which can hamper trait retrieval (Blackburn, 2007). Wavelet analysis overcomes this problem by decomposing the spectral signal into components that relate to different scales linked to the different leaf constituents or traits. We first used the same settings as described in Kattenborn et al. (2019), with the exception of the LUT size (50000) and the parameter range for LUT computation (Cab: 1–75 μg cm^{-2}, Car: 1–15 μg cm^{-2}, Ant: 0.1–4 μg cm^{-2}, Cbrown: 0–1, Ns: 1–3, EWT: 5–51 mg cm^{-2} and LMA: 1–21 mg cm^{-2}). The parameter ranges were largely based on the expected range for herbaceous and shrub species (cf. Feilhauer et al., 2017). The used range has furthermore shown to be optimal for LMA and EWT retrieval through PROSPECT-D inversion across the common species in our study area (Helsen et al., 2020). This approach was termed the 'uncoupled wavelet inversion'. Fourth, we also performed a 'coupled wavelet inversion', with LUT computation for LMA directly coupled to that of EWT, using a conversion factor (f) for each LUT entry, so that each LUT entry for LMA equalled EWT / f. This follows the suggestion of Kattenborn et al. (2017) and has shown to increase LMA estimation accuracy by preventing unrealistic LUT entries (e.g. combined high LMA and low EWT). For each LUT entry, f was randomly sampled within a range of 2.5 and 5. Fifth, we applied the 'hybrid inversion method' combining LUT creation and random forests regression following the approach of Feilhauer et al. (2017), using the same parameter range for LUT computation as described for the 'wavelet inversion method' and a LUT size of 11000.

2.3. Statistical model-based trait estimation

We evaluated the performance of the multibiome partial least square regression (PLSR) model for LMA of Serbin et al. (2019), henceforth termed the 'multibiome LMA model', at the intraspecific level for our four study species. PLSR is a variance-based regression technique that uses covariance structures (components) derived from the predictors (spectral bands) (Abdi, 2003). PLSR reduces the number of predictors by constructing a limited number of components, while at the same time maximizing their covariance with the response variable (Abdi, 2003). Note that the multibiome LMA model parameters were obtained from the supplementary material of Serbin et al. (2019), and that only the Belgian samples were used for the *Rosa rugosa* model.

Additionally, we fit several PLSR models ourselves using the measured LMA, LDMC and EWT, and the collected leaf reflectance data using the 'pls' R package version 2.7–2 (Mevik et al., 2019). A separate PLSR model was trained for each species × trait combination. Note that for the *Rosa rugosa* models, only the Belgian samples were used. Each species dataset was randomly split once in a training and a test dataset (consistent 0.5:0.5 ratio). A PLSR model was then built using the training dataset. To allow optimal comparison with the multibiome LMA model, we used the same PLSR optimization protocol as Serbin et al. (2019), thus identifying the optimal number of PLS components for each model based on the minimal prediction residual sum of squares (PRESS) statistic, as detailed in Serbin et al. (2014). These models are henceforth termed the 'PRESS PLSR models'. More specifically, we calculated the PRESS statistic of successive PLS components through 10-fold cross-validation (CV). This CV approach was jackknifed 30 times. Using this output we determined the optimal number of PLS components as the model with the lowest root mean square error (RMSE) of the PRESS

Table 1
Trait data (dataset size (N), mean value and coefficient of variation (CV, %)) and model accuracy assessment parameters (R^2/NRMSE/VEcv (%)) for the coupled wavelet PROSPECT-D inversion method, the multibiome LMA model and the species-specific RMSEP PLSR models. Test dataset size for all models was N/2. Note that LDMC was indirectly derived for PROSPECT-D by using LMA and EWT estimations. EWT = equivalent water thickness, LDMC = leaf dry matter content, LMA = leaf mass per area.

		Trait data			PROSPECT-D (wavelet, coupled)			PLSR (multibiome LMA model)			PLSR (species-specific, RMSEP model)		
trait	species	N	Mean	CV	R^2	NRMSE	VEcv	R^2	NRMSE	VEcv	R^2	NRMSE	VEcv
LMA	*Rosa rugosa* (BE)	371	9.93	16.1	71.9	46.2	0	80.0	45.3	0	85.8	6.1	85.2
	Rubus caesius	669	5.45	24.7	73.5	33.4	0	76.9	47.1	0	88.4	8.9	88.4
	Jacobaea vulgaris	657	3.77	26.6	31.1	90.9	0	61.8	38.8	0	86.0	10.1	85.7
	Hieracium umbellatum	344	5.40	26.5	37.1	56.2	0	65.2	28.5	0	87.5	10.0	87.0
LDMC	*Rosa rugosa* (BE)	371	0.370	7.7	0.1	8.9	0				69.2	4.6	67.6
	Rubus caesius	669	0.342	12.2	6.0	16.6	0				79.7	5.8	79.7
	Jacobaea vulgaris	657	0.134	19.4	3.4	192.3	0				89.1	6.4	89.1
	Hieracium umbellatum	344	0.166	17.6	0.2	140.0	0				80.8	8.2	79.5
EWT	*Rosa rugosa* (BE)	371	16.85	13.6	59.6	28.0	0				70.4	7.3	69.3
	Rubus caesius	669	10.33	16.9	68.3	43.2	0				81.1	7.9	81.0
	Jacobaea vulgaris	657	24.22	17.5	69.2	16.5	14.0				73.8	9.2	73.2
	Hieracium umbellatum	344	26.94	18.7	66.3	22.2	0				76.2	9.7	76.0

statistic and when successive PLS components did not improve this RMSE, as assessed using a *t*-test on the jackknifed data. Note that unlike Serbin et al. (2019), we did not square root transform the trait data, since all individual species × trait data were normally distributed.

We additionally used a second PLSR optimization approach, using the built-in function 'selectNcomp' ('randomization' method with nperm = 1000 and alpha = 0.05) of the 'pls' R package (i.e. 'RMSEP PLSR models'). This approach selects the optimal number of PLS components based on the minimum RMSEP (prediction error) of the 10-fold CV, which tends to present more conservative results (i.e. less selected components) than the PRESS PLSR models. For the final PRESS PLSR models, we calculated the variable importance in projections (VIP) statistic to visualise the spectral regions used by each trait prediction model.

2.4. Model accuracy assessment

For all trait estimation approaches, model accuracy was evaluated for each species × trait combination separately by performing a linear regression between the observed (y_i) and model-predicted ($\hat{y}_i$) trait values, and calculating the 'variance explained by the predictive model based on cross-validation' (VEcv), the root mean square error (RMSE) and the RMSE normalized (divided) by the mean observed trait value ($\bar{y}_i$) (NRMSE).

For each linear regression model, we quantified the coefficient of determination (R^2), and the intercept (β_0) and slope (β_1), the latter two as proxies of the additive and multiplicative estimation bias, respectively. For β_0, we assessed if values differed significantly from zero based on the standard linear regression output. For β_1, significance of deviation from one was inferred using the 'linearHypothesis' function of the 'car' R package by comparing the linear regression model using β_1 as slope with a similar model using a slope of 1 (Fox and Weisberg, 2019). While R^2 quantifies the percentage of variance explained by the fitted correlation between the observed and predicted traits ($y_i = \beta_1\hat{y}_i + \beta_0$), VEcv represents a true measure of model accuracy, directly quantifying the percentage explained variance in y_i by $\hat{y}_i$ ($y_i = 1\hat{y}_i + 0$) (Li, 2017). The VEcv was calculated using the 'spm' R package as $(1 - (\sum_1^n (y_i - \hat{y}_i)^2 / \sum_1^n \left(y_i - \bar{y}_i\right)^2))100(\%)$ (Li, 2019), with n = the number of observations. Throughout the manuscript 'correlation accuracy' and 'predictive accuracy' refer to R^2 and VEcv, respectively. RMSE and NRMSE present error measures and express the absolute and percentage of residual variance remaining between y_i and $\hat{y}_i$, respectively (Li, 2017). Note that all accuracy assessments were performed on half of the dataset (test datasets).

For the PROSPECT-inversion method that produced the highest trait predictive accuracy, the overall goodness of fit was also assessed for the spectrum of each leaf, based on the absolute deviance (error) of the measured spectrum and the corresponding LUT spectrum.

2.5. PLSR model transferability

To evaluate the generalizability of the final optimal PLSR models, the species-specific optimized PRESS and RMSEP PLSR models were applied across each of the other study species separately. Each of these species-specific models was additionally applied to the *Rosa rugosa* dataset from the species' native range in Japan.

2.6. Trade-off between PLSR training dataset size and model accuracy

To assess the trade-off between training dataset size and model accuracy, each RMSEP PLSR model was performed at different training dataset sizes ranging between 20 and 160 data points at a 20 data point interval. For each of these eight dataset size intervals, data points were randomly selected from the full dataset for both a training and test dataset and each resulting model was optimised following the previously explained minimum RMSEP approach ('randomization' method). This resampling with replacement (bootstrapping) was performed a 100 times for each dataset size interval, allowing the construction of 95% confidence intervals (CIs) for the difference in VEcv and R^2 of each dataset size interval compared to, respectively, the VEcv and R^2 of the 'optimal RMSEP PLSR models'.

3. Results

On average across all study species, ITV was highest for LMA (23.45%) and lowest for LDMC (14.23%) (Table 1). Across all traits, the shrubs *R. rugosa* and *R. caesius* showed lower trait variation (CV) than the herbs *J. vulgaris* and *H. umbellatum* (Table 1, Fig. S1).

Of all tested PROSPECT-D inversion methods, the coupled wavelet inversion method produced the best, albeit only moderately accurate estimations for EWT across all species based on R^2 ($R^2 > 59\%$), although the modified direct inversion method produced equally accurate EWT estimation for two of the four study species (Table 1, S2). LMA correlation accuracy was relatively high for both shrubs ($R^2 > 71\%$) based on the coupled wavelet inversion method (Table 1). However, it was quite low for the two herbs ($R^2 < 40\%$), with higher correlation accuracy based on the modified direct inversion method for *J. vulgaris* (R^2 = 61.1%) and based on the hybrid inversion method for *H. umbellatum* (R^2 = 44.4%) (Table 1, S2). Also for *R. caesius*, correlation accuracy was slightly higher for the modified direct inversion ($R^2 = 77.0\%$) compared to the coupled wavelet inversion (R^2 = 73.5%). Indirect estimation of LMDC based on PROSPECT-D predicted LMA and EWT values did not

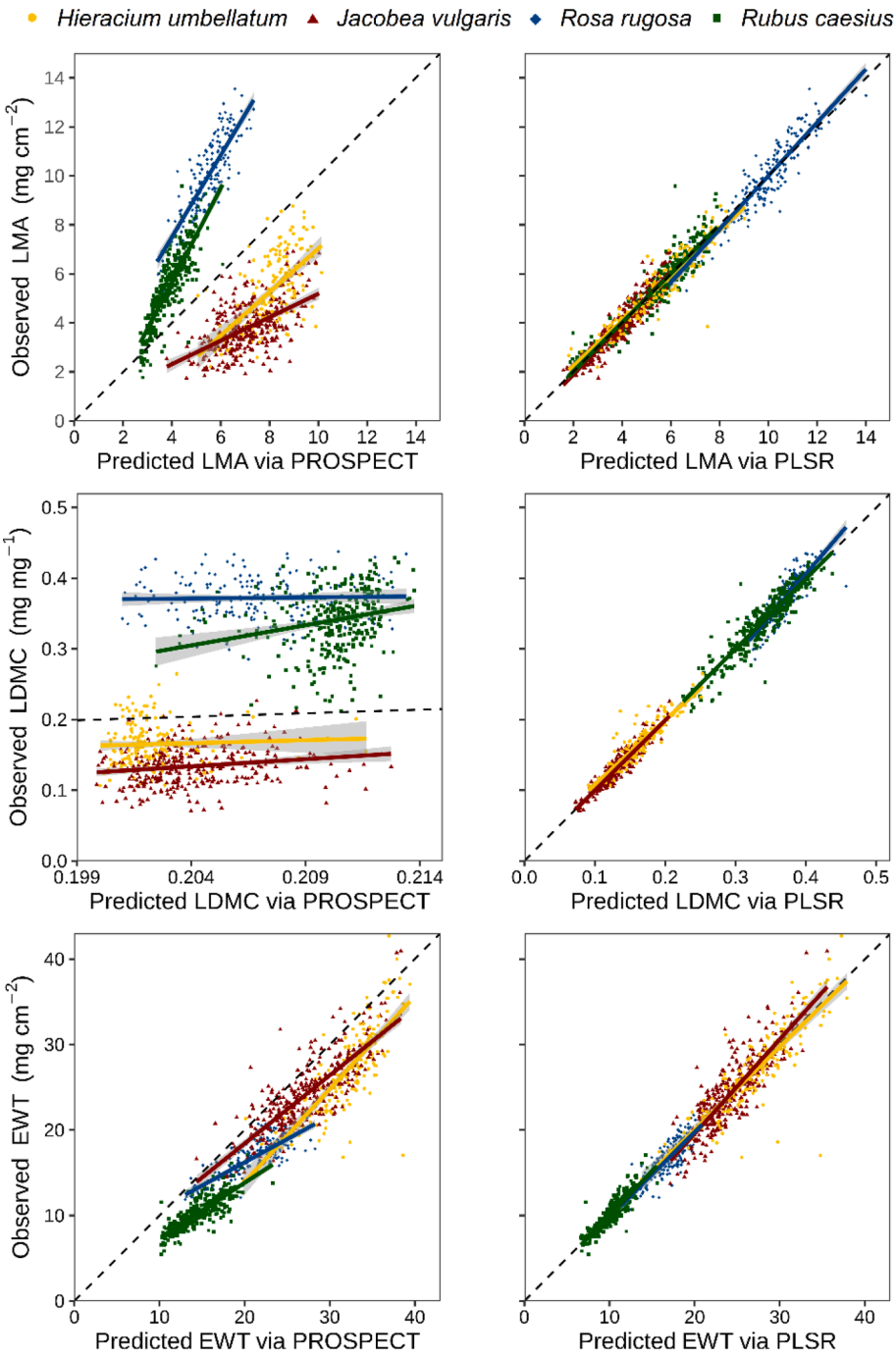

Fig. 1. Correlation scatterplot between predicted and observed trait values based on the PLSR validation datasets (N/2) for the coupled wavelet PROSPECT-D model inversion and the RMSEP PLSR model for each species – trait combination separately. The dotted line visualizes perfect trait predication (Y = X). For PROSPECT-D 'predicted' LDMC values were calculated from the predicted LMA and EWT values. EWT = equivalent water thickness, LDMC = leaf dry matter content, LMA = leaf mass per area.

present accurate results (R^2 < 5%) (Table 1). For most PROSPECT-D predicted trait values, actual predictive accuracy (VEcv) was zero and RMSE and NRMSE (17–91%) quite high (Table 1, S2). Fig. 1 furthermore shows a systematic underestimation of LMA for the shrubs ($\beta_1 > 1$) and overestimation for the herbs ($\beta_1 < 1$) (Table S2). This systematic bias actually resulted in higher NRMSE for PROSPECT-D inversion methods with high correlation accuracy than those with low R^2 values (Table S2).

The mean absolute error between the measured and simulated spectra using the coupled wavelet inversion was relatively low at 0.0169 reflectance units. Although some stronger biases occurred in the visible (±550 nm) and red-edge (±750 nm) regions of the spectra, the spectral regions mainly important for LMA and EWT estimation in the near-infrared and shortwave infrared did not show strong errors, thus indicating relatively robust trait estimations (Fig. S3).

The multibiome LMA model showed higher correlation accuracy than PROSPECT-D inversion for all species, with moderate correlation accuracy for the herbs (R^2 > 61%), and relatively high correlation accuracy for the shrubs (R^2 > 76%) (Table 1, Fig. 2). However, VEcv values were again zero and (N) RMSE high (28–47%), indicating poor predictive accuracy (Table S4). Interestingly, similar underestimation of shrub species LMA observed for PROSPECT-D inversion was present for the multibiome LMA model, next to overestimation of herbaceous species LMA with values > 6 mg cm^{-2}, as also reflected in the β_1 values (Figs. 1–2, Table S4). Although the PLSR coefficients (band importance) for the multibiome LMA model did contain parts of the spectral regions used by the PROSPECT-D model, they also included several seemingly unrelated spectral regions (Fig. 3).

Both the species-specific PRESS and RMSEP PLSR models had high

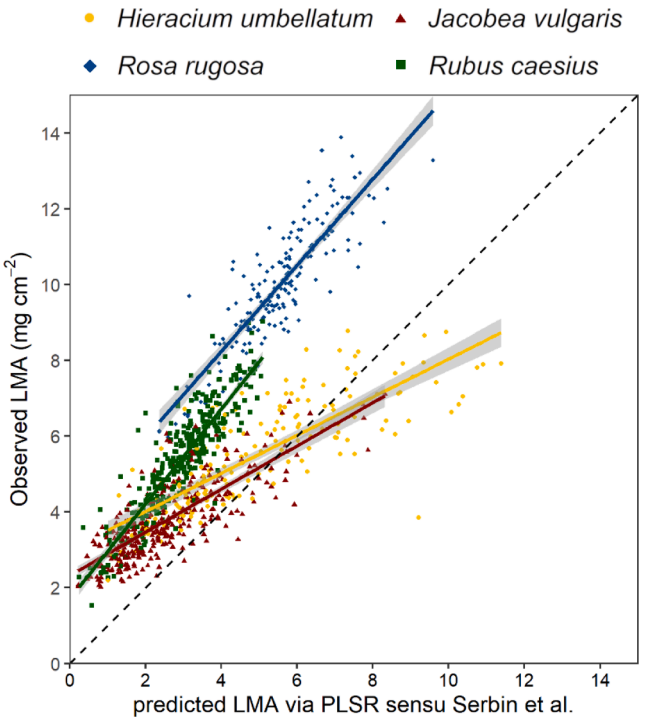

Fig. 2. Correlation scatterplot between predicted and observed trait values based on the PLSR validation datasets (N/2) for the multibiome leaf mass per area (LMA) model for each species separately. The dotted line visualizes perfect trait prediction (Y = X).

model accuracy across all trait × species combinations, with NRMSE below 10% and both R^2 and VEcv above 70% for most models, and above 80% for all LMA and several LDMC models (Table 1, Fig. 1, Table S4). Similarly as for PROSPECT-D inversion, estimations for EWT were slightly less accurate than for LMA (and LDMC) (Table 1). Although the PRESS PLSR models showed somewhat higher model accuracy for several trait × species combinations, their generalizability across species was much lower than that of the RMSEP PLSR models (Tables S5–S6). These results, together with the consistently higher number of PLS components suggest that the PRESS PLSR models suffer from slight overfitting issues and thus that the RMSEP PLSR models are more robust.

The final RMSEP PLSR models for Belgian *R. rugosa* samples nonetheless had relatively low model accuracy for Japanese *R. rugosa* samples. Although NMRSE was below 11% for all traits and the R^2 was around 74% for the LMA model, for LDMC and EWT, the R^2 was only around 50% (Table 2). The Japanese *R. rugosa* samples did however show slightly lower trait means (LMA = 9.11 mg cm^{-2}, EWT = 16.50 mg cm^{-2}, LDMC = 0.356 mg mg^{-1}) and trait variation (CV of LMA = 14.39%, EWT = 12.49%, LDMC = 7.21%) than the Belgian *R. rugosa* samples (Table 1). Similarly, the Belgian *R. rugosa* RMSEP PLSR models did not consistently present high predictive accuracy for the other three study species, with often much lower VEcv than R^2 values (Table 2). Also the final RMSEP PLSR models for the other three study species showed mixed transferability (Table S5). Across the two herbs, all but one of the reciprocally transferred models were highly accurate, with R^2 values ≥ 80% (Table S5). These trait models had relatively similar VIP values (Fig. 3). For *R. rugosa* and *R. caesius*, VIP values of the LMA and EWT models were quite different, but relatively similar for the LDMC model (Fig. 3).

RMSEP PLSR model VEcv and R^2 showed high variance for the two smallest sample size groups (N = 20 and 40) across all trait × species combinations (Figs. 4 & S7). The minimum sample size needed to obtain VEcv values with a maximum difference of 10% to the VEcv of the optimal model on the full dataset (|beta| ⟨10) was higher for the shrubs than the herbs for LMA (N = 80 vs. 60) (Table S8). For LDMC and EWT, this minimum sample size was species-specific, with N = 140, 120, 120 and 60 for LDMC and N = 100, 120, 60 and 40 for EWT, for respectively, *R. rugosa*, *R. caesius*, *J. vulgaris* and *H. umbellatum* (Table S8). To obtain a beta < 5%, even higher sample sizes are needed, in case of LMA and LDMC of *R. rugosa* and LDMC and EWT of *R. caesius* even more than the maximum tested value (N = 160) (Table S8).

4. Discussion

4.1. Performance of the PROSPECT-D and multibiome LMA model

The PROSPECT-D model inversion in our study showed similar LMA correlation accuracy for *R. rugosa* and *R. caesius*, as observed by Helsen et al. (2020) at the interspecific level in our study area (68.6%). These accuracies are furthermore in line with those for LMA retrieval through PROSPECT-inversion of several multispecies (tree) datasets, in respect to R^2, but not RMSE (e.g. Li & Wang, 2011; Cheng et al., 2014; Féret et al., 2019). The much higher RMSE values in our study are due to the systematic underestimation of LMA for both shrub species. The multibiome LMA (PLSR) model showed somewhat higher correlation accuracy (R^2 > 76%) for both shrub study species, and acceptable accuracy for the herbaceous study species (R^2 > 61%), which are in the range of the correlation accuracy of the multibiome LMA model across two independent mixed-species datasets (R^2 = 66%) performed by Serbin et al. (2019). These accuracy levels were nonetheless lower than across the full multibiome calibration dataset (R^2 = 89%) (Serbin et al., 2019). These differences in trait retrieval accuracy between woody and herbaceous species might be partly caused by the relatively low amount of herbaceous grassland species compared to woody species in the calibration datasets for both methods (Féret et al., 2017; Serbin et al., 2019), which might suggest the potential of improving both models by recalibration using more (herbaceous) grass- and shrubland species. In general, spectral leaf-trait retrieval has focused more on woody species and forest biomes (Homolová et al., 2013; Van Cleemput et al., 2018).

Interestingly, in both the multibiome LMA model and the PROSPECT inversions, LMA was systematically overestimated for the two shrubs, but not the two herbs (Figs. 1–2). Although there was some overlap between the spectral regions used by both models, several additional spectral regions were used in the multibiome LMA model (Fig. 3a). Assuming that PROSPECT-D represents the best available knowledge on absorption of LMA structural components, this discrepancy suggests that the multibiome model does not solely rely on (known) mechanistic relationships between LMA components and leaf reflectance, but is additionally, partly calibrated on spectrally detectable trait intercorrelations acting across their global calibration dataset.

Unlike for LMA, for EWT, PROSPECT-D trait estimation had more similar correlation accuracy for shrubs and herbs (R^2 = 60–69%, Table 1). However, the EWT correlation accuracy was noticeably lower than across species in the study area (interspecific R^2 = 80.6%) (Helsen et al., 2020), but still in the range of that of previous work on PROSPECT-inversion based EWT estimation (Li & Wang, 2011). Although the estimation errors for PROSPECT-D could be considered moderate for both LMA and EWT, they get extremely exaggerated when used to calculate LDMC (Fig. 1), thus indicating that PROSPECT-D could not be used to estimate LDMC at the intraspecific level in this study. Some methodological differences between our study and the data used to develop PROSPECT and the multibiome LMA model, such as the smoothing performed on our spectra, might have resulted in lower model accuracies. Specifically for PROSPECT, the use of bidirectional reflectance in our study, as opposed to directional-hemispherical reflectance will likely have affected our results.

4.2. Performance of species-specific (RMSEP) PLSR models

For LMA, correlation accuracy in our study (R^2 > 85%) was in the

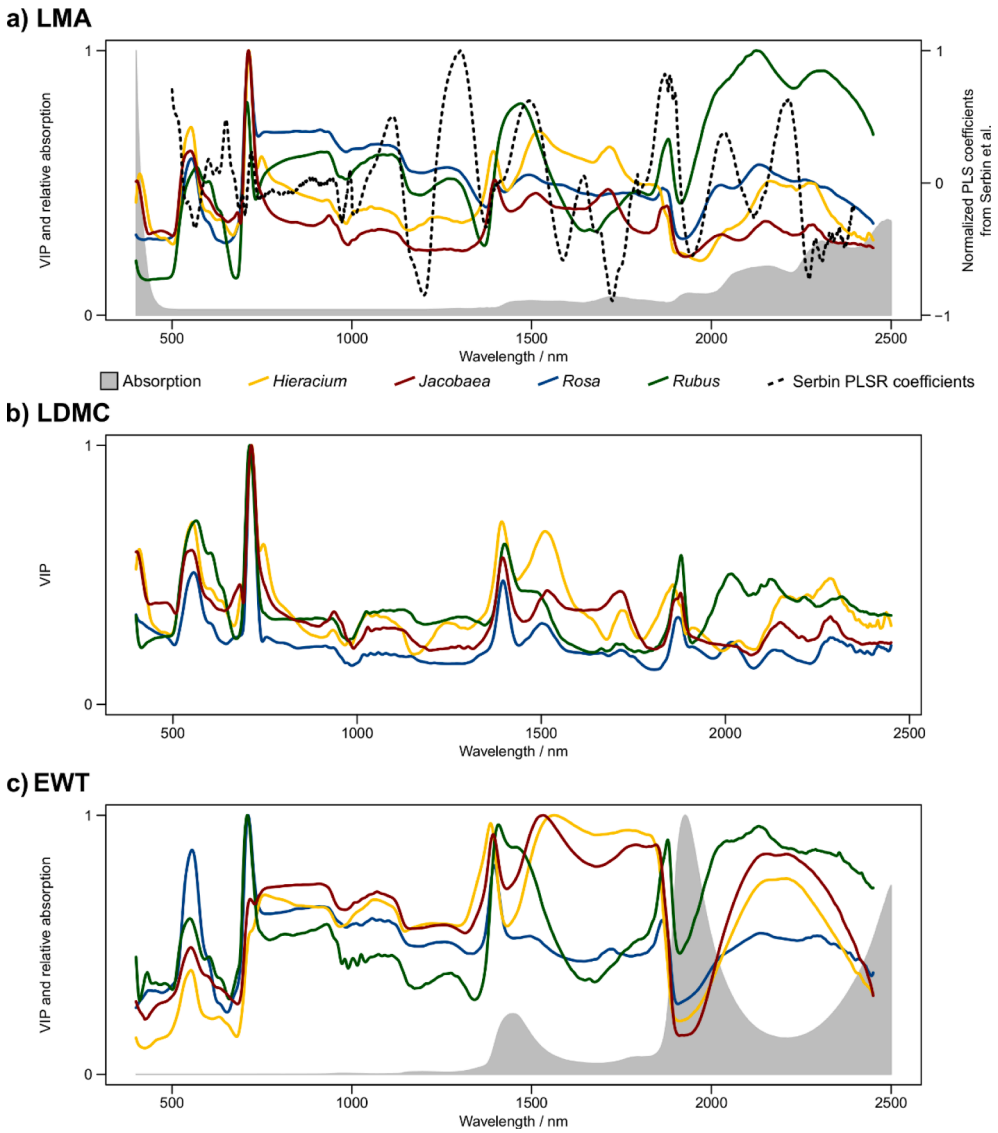

Fig. 3. Variable importance in projections (VIP) statistic for the different RMSEP PLSR models for (a) leaf mass per area (LMA), (b) leaf dry matter content (LDMC) and (c) equivalent water thickness (EWT). Band importance (PLS coefficients) additionally illustrated for the multibiome LMA model of Serbin et al. (2019). Spectral absorption intensity also provided for dry matter (LMA) and water (EWT), as incorporated in the PROSPECT-D radiative transfer model.

Table 2
Model transferability results. Accuracy assessment parameters (R^2/NRMSE/VEcv (%)) for the RMSEP PLSR model constructed for the Belgian (BE) *Rosa rugosa* dataset across all other study species, including the Japanese (JP) *Rosa rugosa* dataset for each trait separately. Test dataset size was N. EWT = equivalent water thickness, LDMC = leaf dry matter content, LMA = leaf mass per area.

		R. rugosa RMSEP PLSR model		
trait	species	R^2	NRMSE	VEcv
LMA	*Rosa rugosa* (JP)	74.1	8.3	66.3
	Rubus caesius	75.6	33.4	0
	Jacobaea vulgaris	49.0	125.3	0
	Hieracium umbellatum	59.4	124.0	0
LDMC	*Rosa rugosa* (JP)	46.7	5.5	41.1
	Rubus caesius	66.4	7.1	66.1
	Jacobaea vulgaris	51.0	58.9	0
	Hieracium umbellatum	53.3	31.8	0
EWT	*Rosa rugosa* (JP)	52.3	10.3	32.4
	Rubus caesius	49.5	39.6	0
	Jacobaea vulgaris	67.0	10.6	63.1
	Hieracium umbellatum	72.8	12.5	55.4

same range as for the previously described multibiome LMA model (Serbin et al., 2019). The only other study assessing LMA from leaf-level spectra for shrub vegetation used simple VIs, which resulted in low correlation accuracy (R^2 = 15%) (Ball et al., 2015). Similarly, Roelofsen et al. (2014) found an accuracy of only 11% for LMA reflectance retrieval with PLSR across 31 herbaceous species and Girard et al. (2020) found a correlation accuracy of 46% for PLSR-based LMA retrieval across 3 shrub and 1 herb species. The latter two study furthermore found a correlation accuracy of 57% and 70%, respectively for LDMC for the same datasets, which is slightly lower than observed at the intraspecific level in our study (R^2 = 69–89%). Girard et al. (2020) also found a correlation accuracy of 71% for EWT retrieval across their 4 study species. Two studies that explored leaf water through PLSR on ground-based canopy measurements, also showed correlation accuracy within the same range as our study (R^2 > 70%) for hay meadows (R^2 = 81%) (Fava et al., 2010) and for heath and dry grasslands (R^2 = 56%) (Roelofsen et al., 2013). Overall these results illustrate that PLSR is a powerful tool, able to retrieve LMA, LDMC and EWT with equally high accuracy at the intraspecific, as at the interspecific and community level.

Note that EWT on rehydrated leaves expresses the maximum water content of leaves, and thus reflects a fixed functional trait value of the

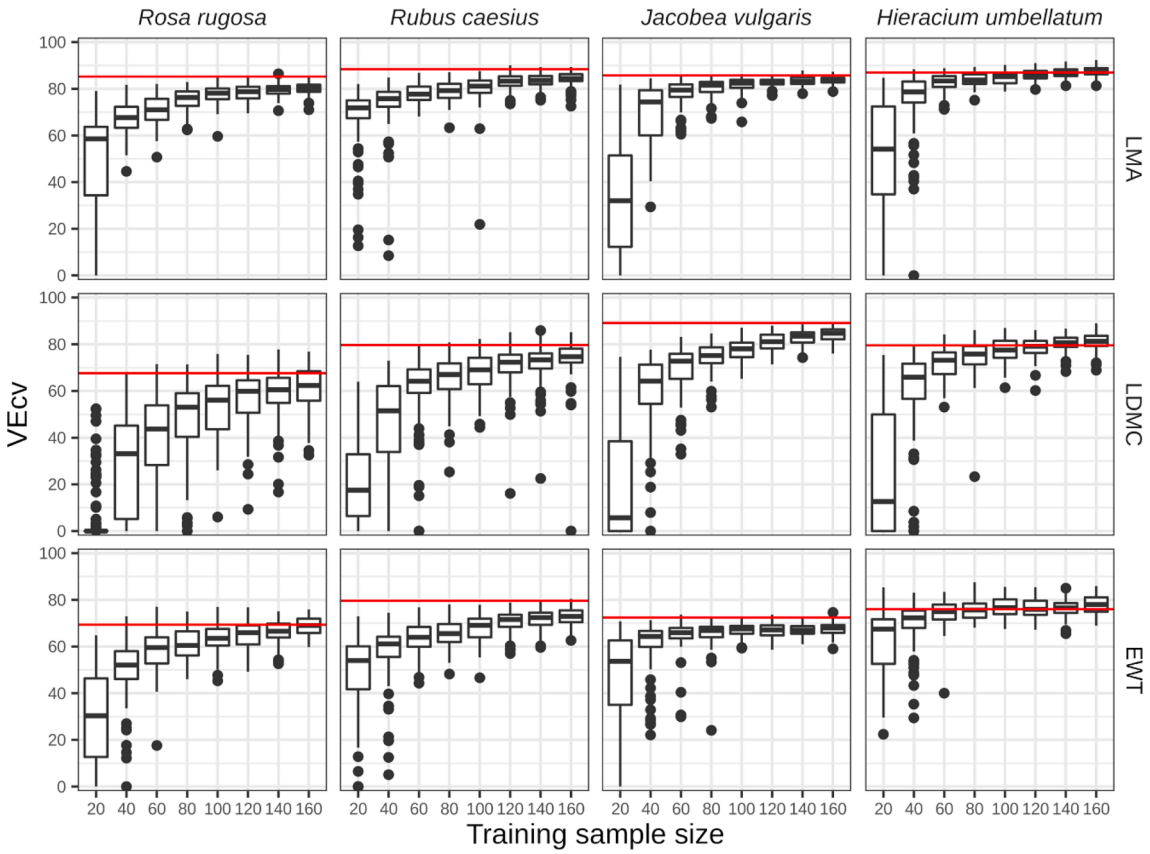

Fig. 4. Boxplots for the predictive accuracy (VEcv) of the RMSEP PLSR models for each species, trait and sample size interval based on 100 bootstraps. The red line shows the VEcv of each PLSR model performed on the full dataset (see Table 1 for dataset sizes). EWT = equivalent water thickness, LDMC = leaf dry matter content, LMA = leaf mass per area.

leaf. For certain applications, such as fire risk assessments, water content is actually measured in the field on partly dehydrated leaves, thus reflecting the water content during certain conditions. If spectral retrieval of EWT by our PLSR models is, similarly as by PROSPECT inversion, largely based on spectral regions directly affected by water content, these models should perform equally well for assessing 'EWT' of partly dehydrated leaves. However, our models should first be tested for field-based 'EWT' assessment of partly dehydrated leaves, before being applied in the context of fire-risk assessment.

4.3. (RMSEP) PLSR model transferability

Despite the high model accuracies, the species-specific transferability success was mixed. Most strikingly, model transferability from the Belgian to the Japanese *R. rugosa* samples was reduced with 12, 23 and 18% for LMA, LDMC and EWT, respectively. Although the trait ranges for LMA, LDMC and EWT were slightly different between Belgium and Japan (Fig. S8), transferability is more likely hampered due to differences in other, unmeasured traits. Indeed, the selected spectral bands of the *R. rugosa* PLSR models suggest that for LMA and EWT the models are partly calibrated on spectrally detectable trait intercorrelations, rather than on spectral regions directly affected by LMA components.

Interestingly, model transferability was much higher within, than across life forms for LMA and LDMC, with $R^2 > 82\%$ and VEcv > 58% for herbaceous species. Transferability did not seem to be related to trait range overlap though, except potentially for LDMC of both herbs (Fig. S8). Spectral retrieval of LDMC and LMA is effectuated by an aggregate of multiple leaf constituents or components, such as leaf proteins, cellulose, lignin and starch (Kattenborn et al., 2019). This was reflected in our LDMC PLSR models, where previously identified absorption bands of these structural components (summarized in Serbin et al., 2014) are represented by high VIP values. For the LMA models, not all absorption features were clearly related to known relevant leaf constituents. The VIP values of the LMA models furthermore showed a more similar pattern within, than among life forms (shrubs and herbs). For EWT the transferability trends were also less clear, suggesting stronger species-dependence of the models. Here, only the shrub species models showed clearly higher VIP for the 1450 and 1950 nm water absorption bands. Our life form dependent transferability results might suggest that the importance of the different structural components for LMA and LDMC are fundamentally different between herbaceous and woody species, potentially also partly explaining the LMA retrieval differences between both life forms for PROSPECT-D and the multibiome LMA model. Alternatively, intercorrelations between other spectrally detectable leaf properties, which differ fundamentally between life forms, are driving the patterns through the different VIP values for the PLSR models across both life forms (Roelofsen et al., 2014). This would suggest that the models are not fully following the physical theory of light absorption due to leaf dry matter components and water. Transferability of our models should ideally be tested across a larger set of herbs and shrubs to assess the generality of these conclusions.

4.4. Trade-off between PLSR training dataset size and model accuracy

The analyses across different test dataset sizes showed that a relatively high number of observations is needed for all trait × species combinations. Although smaller sample sizes were sufficient for LMA compared to the other traits, and for herbs compared to shrubs, our results suggest a minimum of 100–120 leaf samples to obtain robust and accurate species-specific PLSR models. High intraspecific trait variability (ITV) (Table 1) seemed to result in a lower minimum needed test

dataset size, likely explaining the lower sample sizes needed for LMA compared to LMDC. Across all techniques, LMA was clearly the easiest trait to predict. This is reflected in higher predictive accuracy, higher transferability and smaller needed minimum test dataset sizes. Note that our resampling strategy did not directly account for trait range. As such, small sample sizes will often result in reduced trait ranges of the validation dataset, and thus potentially lower accuracy than would be observed when resampling using a fixed trait range (Schweiger, 2020). However, this presents the most likely scenario during real data collection, where the full extent of the intraspecific trait range will be unknown before analysis.

5. Conclusions

Although the PROSPECT-D model inversion and the multibiome LMA PLSR model were quite accurate in intraspecific LMA predictions for shrubs, their performance was lower for herbs, potentially due to limited herbaceous species in their original calibration datasets. PROSPECT-D was furthermore slightly less successful in retrieving EWT at the intraspecific level. The use of bidirectional reflectance in our study likely resulted in lower PROSPECT inversion accuracy. Despite the reasonably strong correlation accuracy (R^2), true predictive accuracy (VEcv) was very low for most species × trait combinations, indicating the importance of species-specific, or potentially only life form-specific (e.g. shrubs and herbs) correction factors addressing the additive and multiplicative estimation biases.

If high predictive accuracy is needed for LMA, LDMC or EWT, we suggest that species- (and range-) specific (RMSEP) PLSR models are built, since this clearly allows higher predictive accuracy. Although transferability of species-specific PLSR models was limited between certain species, our results nonetheless point in the direction of potentially high transferability among herbaceous species, although this should be tested more widely in the future. The construction of species-specific PLSR models comes at the cost of a relatively large needed sample size of 60–160 leaves however, depending on the trait.

6. Data accessibility

Leaf-level spectral and trait data are available from respectively the EcoSIS spectral library (https://ecosis.org/package/e88b832d-d7da-48b5-af59-25a8079a0ab6) and the TRY Plant Trait Database (https://www.try-db.org/). An R script allowing to run our different species × trait level RMSEP PLSR models is furthermore available on https://github.com/LeonardoUU/Helsen-Bassi_et_al_2021_ecological_indicators.

CRediT authorship contribution statement

Kenny Helsen: Conceptualization, Investigation, Formal analysis, Writing – original draft, Visualization. **Leonardo Bassi:** Conceptualization, Investigation, Methodology, Formal analysis, Writing – original draft, Visualization. **Hannes Feilhauer:** Methodology, Software, Writing - review & editing, Visualization. **Teja Kattenborn:** Methodology, Software, Writing - review & editing. **Hajime Matsushima:** Resources, Investigation. **Elisa Van Cleemput:** Methodology, Software, Investigation, Writing - review & editing. **Ben Somers:** Resources, Writing - review & editing, Supervision. **Olivier Honnay:** Writing - review & editing, Supervision.

Declaration of Competing Interest

The authors declare that they have no known competing financial interests or personal relationships that could have appeared to influence the work reported in this paper.

Acknowledgements

We thank Stijn Cornelis and Kasper Van Acker for help in the field, and Hannelore Theetaert and VLIZ (Vlaams Instituut voor de Zee) for logistic support in the MSO (Marien Station Oostende), ANB Kust-Polders for field permits in Belgium and Jean-Baptiste Féret for assistance with data analysis. This paper was written when K.H. held a postdoc fellowship (1202817N) and received a travel grant for a short study visit to Hokkaido (K210519N) of the Flemish Fund for Scientific Research (FWO).

Appendix A. Supplementary data

Supplementary data to this article can be found online at https://doi.org/10.1016/j.ecolind.2021.108111.

References

Abdi, H., 2003. Partial least square regression (PLS regression). Encycl. Res. Methods Soc. Sci. 6, 792–795.
Ali, A.M., et al., 2017. Specific leaf area estimation from leaf and canopy reflectance through optimization and validation of vegetation indices. Agric. For. Meteorol. 236, 162–174.
Asner, G.P., et al., 2011. Taxonomy and remote sensing of leaf mass per area (LMA) in humid tropical forests. Ecol. Appl. 21, 85–98.
Asner, G.P., et al., 2015. Quantifying forest canopy traits: Imaging spectroscopy versus field survey. Remote Sens. Environ. 158, 15–27.
Atzberger, C., et al., 2015. Comparative analysis of different retrieval methods for mapping grassland leaf area index using airborne imaging spectroscopy. Int. J. Appl. Earth Obs. Geoinf. 43, 19–31.
Ball, A., et al., 2015. Patterns of leaf biochemical and structural properties of Cerrado life forms: Implications for remote sensing. PLoS One 10, 1–15.
Bennett, J.A., et al., 2016. The reciprocal relationship between competition and intraspecific trait variation. J. Ecol. 104, 1410–1420.
Blackburn, G.A., 2007. Wavelet decomposition of hyperspectral data: A novel approach to quantifying pigment concentrations in vegetation. Int. J. Remote Sens. 28, 2831–2855.
Breza, L.C., et al., 2012. Within and between population variation in plant traits predicts ecosystem functions associated with a dominant plant species. Ecol. Evol. 2, 1151–1161.
Bruun, H.H., 2005. Biological flora of the British Isles: *Rosa rugosa* Thunb. ex Murray. J. Ecol. 93, 441–470.
Cheng, T., et al., 2014. Deriving leaf mass per area (LMA) from foliar reflectance across a variety of plant species using continuous wavelet analysis. ISPRS J. Photogramm. Remote Sens. 87, 28–38.
Chun, Y.J., et al., 2009. Comparison of quantitative and molecular genetic variation of native vs. invasive populations of purple loosestrife (*Lythrum salicaria* L., Lythraceae). Mol. Ecol. 18, 3020–3035.
Colombo, R., et al., 2008. Estimation of leaf and canopy water content in poplar plantations by means of hyperspectral indices and inverse modeling. Remote Sens. Environ. 112, 1820–1834.
Fava, F., et al., 2010. Fine-scale assessment of hay meadow productivity and plant diversity in the European Alps using field spectrometric data. Agric. Ecosyst. Environ. 137, 151–157.
Feilhauer, H., et al., 2017. Optical trait indicators for remote sensing of plant species composition: Predictive power and seasonal variability. Ecol. Indic. 73, 825–833.
Feilhauer, H., et al., 2018. Are remotely sensed traits suitable for ecological analysis? A case study of long-term drought effects on leaf mass per area of wetland vegetation. Ecol. Indic. 88, 232–240.
Féret, J.-B., et al., 2008. PROSPECT-4 and 5: Advances in the leaf optical properties model separating photosynthetic pigments. Remote Sens. Environ. 112, 3030–3043.
Féret, J.-B., et al., 2017. PROSPECT-D: towards modeling leaf optical properties through a complete lifecycle. Remote Sens. Environ. 193, 204–215.
Féret, J.-B., et al., 2019. Estimating leaf mass per area and equivalent water thickness based on leaf optical properties: Potential and limitations of physical modeling and machine learning. Remote Sens. Environ. 231, 110959.
Fox, J., Weisberg, S., 2019. An R companion to applied regression, 3rd ed. Sage publications inc., Thousand Oaks, CA, USA.
Gamon, J.A., et al., 2019. Assessing vegetation function with imaging spectroscopy. Surv. Geophys. 40, 489–513.
Garnier, E., et al., 2004. Plant functional markers capture ecosystem properties during secondary succession. Ecology 85, 2630–2637.
Girard, A., et al., 2020. Foliar spectra and traits of bog plants across nitrogen deposition gradients. Remote Sens. 12, 2448.
Helsen, K., et al., 2018. Impact of an invasive alien plant on litter decomposition along a latitudinal gradient. Ecosphere 9, e02097.
Helsen, K., et al., 2020. Optical traits perform equally well as directly-measured functional traits in explaining the impact of an invasive plant on litter decomposition. J. Ecol. 108, 2000–2011.
Hodgson, J.G., et al., 2011. Is leaf dry matter content a better predictor of soil fertility than specific leaf area? Ann. Bot. 108, 1337–1345.

Homolová, L., et al., 2013. Review of optical-based remote sensing for plant trait mapping. Ecol. Complex. 15, 1–16.
Jacquemoud, S., Baret, F., 1990. PROSPECT: A model of leaf optical properties spectra. Remote Sens. Environ. 34, 75–91.
Jacquemoud, S., et al., 2009. PROSPECT + SAIL models: A review of use for vegetation characterization. Remote Sens. Environ. 113, S56–S66.
Jung, V., et al., 2014. Intraspecific trait variability mediates the response of subalpine grassland communities to extreme drought events. J. Ecol. 102, 45–53.
Kattenborn, T., Schmidtlein, S., 2019. Radiative transfer modelling reveals why canopy reflectance follows function. Sci. Rep. 9, 6541.
Kattenborn, T., et al., 2017. Linking plant strategies and plant traits derived by radiative transfer modelling. J. Veg. Sci. 28, 717–727.
Kattenborn, T., et al., 2019. Differentiating plant functional types using reflectance: which traits make the difference? Remote Sens. Ecol. Conserv. 5, 5–19.
Kelager, A., Pedersen, J.S., Bruun, H.H., 2013. Multiple introductions and no loss of genetic diversity: Invasion history of Japanese Rose, *Rosa rugosa*, in Europe. Biol. Invasions 15 (5), 1125–1141.
Kunstler, G., et al., 2016. Plant functional traits have globally consistent effects on competition. Nature 529, 204–207.
Lawlor, D.W., Cornic, G., 2002. Photosynthetic carbon assimilation and associated metabolism in relation to water deficits in higher plants. Plant Cell Environ. 25, 275–294.
Lehnert, L.W., et al., 2018. hsdar: Manage, analyse and simulate hyperspectral data in R. R package version (7), 2.
Li, J., 2019. spm: Spatial predictive modeling. R package version 1.2.0. https://CRAN.R-project.org/package=spm.
Li, J., 2017. Assessing the accuracy of predictive models for numerical data: Not r nor r2, why not? Then what? (Q. Zhang, Ed.), PLoS One 12, e0183250.
Li, P., Wang, Q., 2011. Retrieval of leaf biochemical parameters using PROSPECT inversion: A new approach for alleviating ill-posed problems. - IEEE Trans. Geosci. Remote Sens. 49, 2499–2506.
Messier, J., et al., 2010. How do traits vary across ecological scales? A case for trait-based ecology. Ecol. Lett. 13, 838–848.
Mevik, B.-H. et al., 2019. pls: Partial least squares and principal component regression. R package version 2.7-2. https://CRAN.R-project.org/package=pls.
Pérez-Harguindeguy, N., et al., 2013. New handbook for standardised measurement of plant functional traits worldwide. Aust. J. Bot. 61, 167–234.
Pierce, S., et al., 2017. A global method for calculating plant CSR ecological strategies applied across biomes world-wide. Funct. Ecol. 31, 444–457.
Poorter, H., et al., 2009. Causes and consequences of variation in leaf mass per area (LMA): a meta-analysis. New Phytol. 182, 565–588.
Roelofsen, H.D., et al., 2013. Trait estimation in herbaceous plant assemblages from in situ canopy spectra. Remote Sens. 5, 6323–6345.
Roelofsen, H.D., et al., 2014. Predicting leaf traits of herbaceous species from their spectral characteristics. Ecol. Evol. 4, 706–719.
Savitzky, A., Golay, M.J.E., 1964. Smoothing and differentiation of data by simplified least squares procedures. Anal. Chem. 36, 1627–1639.
Schweiger, A.K., 2020. Spectral field campaigns: planning and data collection. In: Cavender-Bares, J., et al. (Eds.), Remote sensing of plant biodiversity. Springer International Publishing, Cham, pp. 385–423.
Serbin, S.P., et al., 2014. Spectroscopic determination of leaf morphological and biochemical traits for northern temperate and boreal tree species. Ecol. Appl. 24, 1651–1669.
Serbin, S.P., et al., 2019. From the Arctic to the tropics: multibiome prediction of leaf mass per area using leaf reflectance. New Phytol. 224, 1557–1568.
Siefert, A., et al., 2015. A global meta-analysis of the relative extent of intraspecific trait variation in plant communities. Ecol. Lett. 18, 1406–1419.
Singh, A., et al., 2015. Imaging spectroscopy algorithms for mapping canopy foliar chemical and morphological traits and their uncertainties. Ecol. Appl. 25, 2180–2197.
Smart, S.M., et al., 2017. Leaf dry matter content is better at predicting above-ground net primary production than specific leaf area (K Field, Ed.). Funct. Ecol. 31, 1336–1344.
Spafford, L., et al., 2021. Spectral subdomains and prior estimation of leaf structure improves PROSPECT inversion on reflectance or transmittance alone. Remote Sens. Environ. 252, 112176.
Tao, J., Zuo, J., He, Z.e., Wang, Y., Liu, J., Liu, W., Cornelissen, J.H.C., Morriën, E., 2019. Traits including leaf dry matter content and leaf pH dominate over forest soil pH as drivers of litter decomposition among 60 species (E Morriën, Ed.). Funct. Ecol. 33 (9), 1798–1810.
Van Cleemput, E., et al., 2018. The functional characterization of grass- and shrubland ecosystems using hyperspectral remote sensing: trends, accuracy and moderating variables. Remote Sens. Environ. 209, 747–763.
Verrelst, J., et al., 2015. Optical remote sensing and the retrieval of terrestrial vegetation bio-geophysical properties - A review. ISPRS J. Photogramm. Remote Sens. 108, 273–290.
Verrelst, J., et al., 2019. Quantifying vegetation biophysical variables from imaging spectroscopy data: a review on retrieval methods. Surv. Geophys. 40, 589–629.
Wang, L., et al., 2011. Estimating dry matter content from spectral reflectance for green leaves of different species. Int. J. Remote Sens. 32, 7097–7109.
Wellstein, C., et al., 2017. Effects of extreme drought on specific leaf area of grassland species: A meta-analysis of experimental studies in temperate and sub-Mediterranean systems. Glob. Chang. Biol. 23, 2473–2481.
Westoby, M., 1998. A leaf-height-seed (LHS) plant ecology strategy scheme. Plant Soil 199, 213–227.
Wilson, P.J., et al., 1999. Specific leaf area and leaf dry matter content as alternative predictors of plant strategies. New Phytol. 143, 155–162.
Wold, S., et al., 1983. The multivariate calibration problem in chemistry solved by the PLS method. In: Kågström, B., Ruhe, A. (Eds.), Matrix Pencils. Lecture Notes in Mathematics, 973. Springer, Berlin, Heidelberg, pp. 286–293.
Wright, I.J., et al., 2004. The worldwide leaf economics spectrum. Nature 428, 821–827.
Yebra, M., et al., 2013. A global review of remote sensing of live fuel moisture content for fire danger assessment: Moving towards operational products. Remote Sens. Environ. 136, 455–468.
Zeiger, E., 1983. The biology of stomatal guard cells. Annu. Rev. Plant Physiol. 34, 441–475.
Zou, J., et al., 2007. Differences in morphological and physiological traits between native and invasive populations of *Sapium sebiferum*. Funct. Ecol. 21, 721–730.